THE TURBINE DRIVEN ROTOR CONCEPT, A NEW VISION FOR HELICOPTER PROPULSION

Frank Buysschaert*, Simon Newman*, Scott Walker*, Hubert Antoine◊ and Patrick Hendrick‡

* University of Southampton, Faculty of Engineering and the Environment
Aerodynamics and Flight Mechanics Research Group
Highfield Campus, SO17 1BJ, United Kingdom

‡ Université Libre de Bruxelles, Faculté des Sciences Appliquées
Aero-Thermo-Mechanics Laboratory
CP165/41, 50, F.D. Roosevelt Avenue
B-1050 Brussels, Belgium

◊ Sagita
37, Avenue de l'Indépendance
B-4020 Wandre, Belgium

The TDR-helicopter concept is a helicopter configuration with no mechanical transmission, using coaxial rotors driven by a Ljungström turbine. This configuration offers reduced helicopter complexity and weight. Three TDR-helicopter cycles are proposed and examined thermodynamically. The piston engine cycle, using Avgas and diesel, and the turboshaft engine cycle exhibit design cycle specific fuel consumptions that are competitive with conventional helicopters, even though being limited by the Ljungström turbine bearing temperature. However, the turboshaft engine cycle is less attractive because of the need for heat exchangers and the loss of the exhaust gas mass flow. The turbofan cycle does not suffer from this problem and offers the potential to outperform the conventional helicopter, while offering propulsive force in addition.

1 INTRODUCTION

Helicopter design is continually challenged to comply with the various mission requirements of helicopter operators, yet the basic design of the helicopter rarely changes. Except for some exotic configurations, a thermal engine driving the rotor(s) via a mechanical transmission system still represents the majority of the global helicopter fleet. However, it has been shown[1] that the installed thermal engine(s) and the mechanical transmission system are the most vulnerable components of the helicopter.

This paper discusses a new helicopter concept, named TDR or *Turbine Driven Rotor*, a concept which was first revealed by the company Sagita S.A. in 2009[2][3] under the French acronym *REDT* or *Rotor à Entraînement Direct par Turbine*. The concept has coaxial rotors and does not need a mechanical drive system to link the rotors with an internal combustion engine because of the integration of a turbine in the rotorhead. The omission of the drive train is expected to have a direct and positive impact on the total performance of the helicopter[1], i.e. improving safety, reducing cost and removing a part which inherently suffers from mechanical flat rating.

Embedding a turbine in a rotor head to drive coaxial rotors directly is not new, since it was already attempted by Ramme[4] in the late sixties, but its novelty lies with the use of the less complex Ljungström turbine[5] driven by compressed hot air, and the introduction of an independent yaw control system[6] based on circulation control. The hot compressed air driving the turbine is delivered by a combination of an air pressurisation process and the recovery of the exhaust gas thermal energy.

This paper presents three thermodynamic cycles with their concurring TDR-helicopter configuration, which provide the rotor embedded Ljungström turbine (RELT) with hot and pressurised air. In each cycle, a specific kind of internal combustion aero-engine (ICE) is used, viz. :

- Piston Engine : Avgas and Diesel
- Turboshaft engine
- Turbofan engine

Prior to the discussion of these cycles, the general thermodynamic cycle on which the TDR concept is based, will be explained. Finally, the cycles will be compared and their potential evaluated.

FIG. 1 : THE TDR HELICOPTER, COPYRIGHT SAGITA

2 THE LJUNGSTRÖM TURBINE

Conceived in the beginning of the 20th century, the Ljungström turbine was considered to be a revolutionary answer to the steam-leakage plagued and bulky axial steam turbines[7] used in steam turbine plants. The two contra-rotating turbine disks of which the Ljungström turbine consists (Fig. 2), and on which multiple blade stages are put, each drove an electric generator. The radial outflow configuration meant an increasing flow area towards the turbine outlet, conveniently taking care of the increased specific volume of the steam due to its expansion. The result of this setup was a much more compact and efficient steam turbine plant. Indeed, it was indicated to exhibit competitive efficiencies with respect to its counterparts. E.g. Houberechts[8] mentions efficiencies up to 91%.

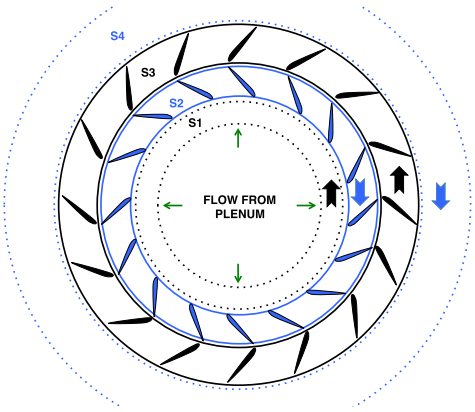

FIG. 2 : THE LJUNGSTRÖM TURBINE - SCHEME RADIAL PLANE

The introduction of powerful gas turbine engines and the heavy investments in axial turbine research in the aeronautical industry made the Ljungström turbine less attractive for stationary configurations. Peng[9] suggested that its disappearance on the market was due to its complexity and cost to manufacture with respect to alternatives. However, its implementation in a helicopter rotor head appears worthy of examination. Indeed, the integration in the helicopter rotor head renders the need for a mechanical transmission between mechanical power source and rotor obsolete. The use of a coaxial rotor when using the Ljungström turbine (RELT) is obvious, consequently offering the benefits of coaxial rotors, such as the potential to improve the performance envelope[10]. The mechanical transmission complexity of coaxial rotors is also no longer an issue, since it is not longer required (Fig. 3). Furthermore, coaxial rotors require less power to airlift the same gross weight, which encourages a thorough examination of the concept[24].

The disadvantage of the RELT is that its isentropic efficiency is expected to be lower than those observed on steam turbines due to the lower Reynolds numbers and the effects of increased secondary losses[5]. Indeed, the blade aspect ratio cannot be high, because this would increase the rotor head drag.

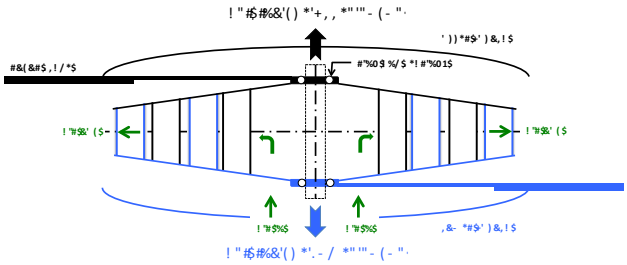

FIG. 3 : THE LJUNGSTRÖM TURBINE - SCHEME AXIAL PLANE

3 THERMODYNAMIC CYCLE STUDY

3.1 The General Cycle

The goal of the TDR-thermodynamic cycles is to condition the gases delivered to the RELT optimally, i.e. to assure high cycle efficiency with a minimum impact on the helicopter empty weight. Defining P_T^* as the power delivered by the RELT to the rotors, and $\dot{Q}_F$ the heat introduced by the combustion of fuel, the thermodynamic cycle efficiency then becomes :

(1) $$\epsilon_{th} = \frac{P_T^*}{\dot{Q}_F}$$

The TDR-thermodynamic cycles are open cycles, as indicated in Fig. 4. Indeed, air with total enthalpy H_{in} is ingested from the atmosphere under a certain temperature and pressure, processed and expelled again with an enthalpy H_{out} while producing work per unit time P_T^* in the RELT.

Unless well thermally insulated, (cold source) heat losses $\dot{Q}_C$ from the system to the surroundings are possible and need to be accounted for in the energy balance. Finally, it is conceivable to introduce a post combustion process, which will introduce heat $\dot{Q}_{PC}$ to the flow prior to entering the RELT, and an immediate expulsion of a fraction of the ICE exhaust gases with enthalpy $\dot{H}_{ex}$ from the TDR-cycle without passing through the RELT. Note that the ICE is considered as an integral part of the thermodynamic cycle.

Applying the first law of thermodynamics on the general thermodynamic TDR-cycle in steady state conditions then yields for the cycle efficiency ϵ_{th} (Fig. 4) :

(2) $$\epsilon_{th} = \frac{(\dot{H}_{in} + \dot{Q}_F + \dot{Q}_{PC}) - (\dot{H}_{out} + \dot{H}_{ex} + \dot{Q}_C)}{\dot{Q}_F + \dot{Q}_{PC}}$$

From Eq.2 it is clear that the right term in the numerator should be minimised. Heat losses $\dot{Q}_C$ must therefore be avoided as well as bleeding ICE exhaust gases. Indeed, one may prove via the second law of thermodynamics that the entropy production of a system expelling exhaust gases directly into the atmosphere is higher than when letting them deliver work first before being expelled. Consequently, $\dot{H}_{ex}$ is

ideally avoided by letting all exhaust gases pass through the RELT.

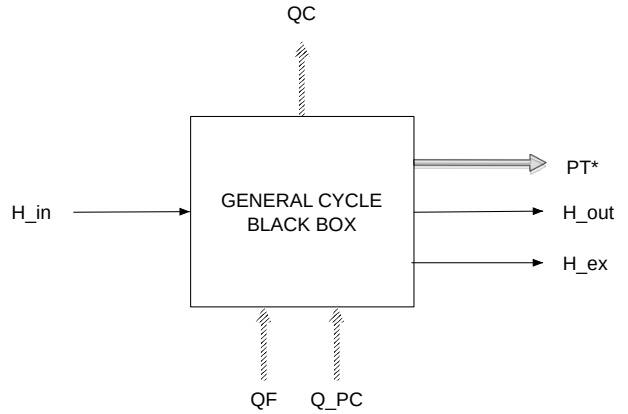

FIG. 4 : THE GENERAL THERMODYNAMIC TDR-CYCLE

What post-combustion concerns, this typically concurs with high system exhaust gas temperatures. Even though this allows more power to be extracted and deliver higher values of P_T^*, limitations are imposed by the RELT material choice (weight) and the maximum temperatures that can be supported by the bearings. In case grease lubricated bearings are installed, the maximum RELT total inlet temperature LTIT is around 400K. Consequently, post-combustion will not be considered.

From the above considerations, it appears that a thermodynamic cycle where all heat and exhaust gases are recovered from the ICE – the latter used to deliver the required power to compress the gases – is most beneficial to the cycle efficiency. Based on this conclusion, three thermodynamic cycles are proposed subsequently, each using a specific type of aero-engine.

3.2 **The Piston Engine TDR-Cycle**

3.2.1 **Cycle performance parameter definition**

The piston engine TDR-cycle uses a piston engine to compress and heat the air before letting it expand through the RELT. Fig. 5 indicates the intended cycle. An air mass flow is ingested from the surroundings through a compressor (C) and is then split. One part is sucked in by the piston engine (PE) and is defined as primary flow $\dot{m}_p$. The other part, or secondary flow $\dot{m}_s$, bypasses the engine and is mixed (MIX) with the PE exhaust gases before entering the turbine. Note that the components in the plenum operate under the pressurised conditions made by the compressor. A shut-off valve (SOV) closes the flow path in case of a system malfunction. The mass flow through the RELT is then stopped, minimising the power losses in autorotation. In case the optimum PE output shaft rotational velocity cannot be matched with the optimum compressor characteristics, a gearbox (GBX) may be required.

Some important performance characteristics of the stated configuration can now be established. Noting from Fig. 6, control volume (CV) 1, P_T^* may be expressed as :

$$P_T^* = \dot{m}_t(h_{t45} - h_{t5}) \tag{3}$$

where $\dot{m}_t$ the total mass flow through the RELT and h_{ti} the total specific enthalpy for section i.

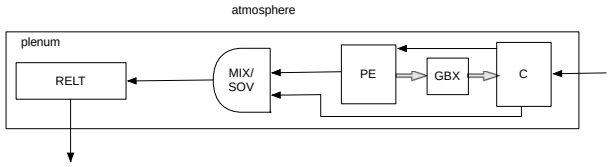

FIG. 5 : THE PISTON ENGINE TDR-CYCLE

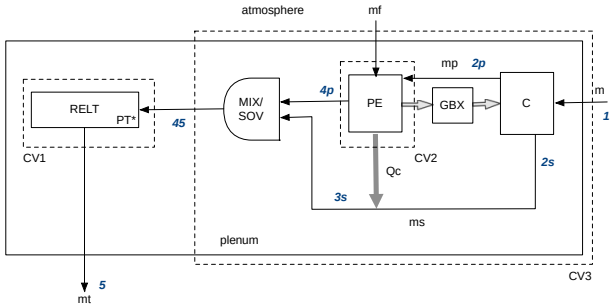

FIG. 6 : THE PISTON ENGINE TDR-CYCLE BREAKDOWN

For a perfect gas, the total enthalpy may be rewritten as $h_t = C_p T_t$. C_p is the heat capacity at constant pressure. Adopting the reasonable assumption that the compression ratio of the compressor π_C equals the expansion ratio over the turbine π_T, Eq.3 can be further developed to :

$$P_T^* = \dot{m}_t C_{pg} T_{t45}\left[1 - \left(\frac{1}{\pi_T}\right)^{\frac{\gamma_g - 1}{\gamma_g}\cdot\eta_{p,T}}\right] \tag{4}$$

where π_T is the expansion ratio over the turbine, γ_g the specific heat ratio of the gases through the RELT (the suffix g stands for the air-exhaust gas mixture) and $\eta_{p,T}$ the polytropic turbine efficiency. The polytropic efficiency is used since it is a better yardstick to reflect the maturity of the used technology[10] and less dependent on pressure ratio. The fuel mass flow $\dot{m}_f$ may be found by analysing CV3 shown in Fig. 6. If $\dot{m}$ is the mass flow entering the compressor, i.e. $\dot{m} = \dot{m}_p + \dot{m}_s$, then $\dot{m}_f$ is approximated by :

$$\dot{m}_f = \frac{\dot{m}(C_{pg}T_{t45} - C_p T_{t1})}{\eta_{CC} LHV} \tag{5}$$

where η_{CC} is the combustion efficiency and LHV the lower heating value of the fuel (Avgas or Diesel, Table 1).

η_{CC} depends on the PE type. Considering the PE to work at the maximum continuous regime, it is possible

to estimate values for η_{CC}. For spark ignition engines (SPI), η_{CC} may be approximated by :

(6) $$\eta_{CC} = \frac{1}{\phi} \qquad \text{(SPI only)}$$

where ϕ is the equivalence ratio :

(7) $$\phi = \frac{FAR}{FAR_{st}}$$

FAR stands for the fuel-to-air ratio and FAR_{st} the fuel-to-air ratio under stoichiometric conditions :

(8) $$FAR = \frac{\dot{m}_f}{\dot{m}_p}$$

If maximum power is required, $\phi \cong 1.8$[11] for SPI, which concurs with an incomplete combustion and produces mainly carbon monoxide and di-hydrogen as combustion products. In case of the maximum continuous operating regime, $\phi \cong 1.5$ is a more conservative value (Table 2). This power setting is likely to occur during flight, since take-off conditions are not continuously required and as a consequence, a lower power setting will be selected, e.g. when flying close to the power bucket[12].

Diesel engines (DE) however are excluded from rich fuel mixtures. The combustion process always requires excess air because the fuel is less easily dispersed in the cylinder than more volatile fuels such as Avgas used in SPI. The maximum performance regime for DE is found near $\phi \cong 0.7$[13]. This is near the smoke-limit. Hence, for the calculations with DE, Eq.6 does not apply. It is then assumed that for the DE : $\eta_{CC} = 0.99$.

The cycle specific fuel consumption SFC now follows from Eq.4 and Eq.5 :

(9) $$SFC = \frac{\dot{m}_f}{P_T^*} = \frac{1 - \frac{C_p}{C_{pg}}\frac{T_{t1}}{T_{t45}}}{\eta_{CC} LHV \left[1 - \left(\frac{1}{\pi_C}\right)^{\frac{\gamma_g - 1}{\gamma_g}\cdot\eta_{p,T}}\right]}$$

Note that SFC depends on non-dimensional parameters only. Note also that here the compression ratio π_C is used as a design parameter instead of the turbine expansion ratio π_T. SFC increases with T_{t45}/T_{t1} as more fuel is required per unit mass expanding through the RELT. Increasing only π_C raises T_{t2}/T_{t1} and decreases SFC (Fig. 7) because when T_{t45}/T_{t1} remains constant, so is $\dot{m}_f/\dot{m}$ and the concurring primary and secondary mass flow fractions. The increase in π_C, will consequently require a lower PE exhaust gas temperature T_{t4p}(Eq.19), and this is only possible with a more efficient PE, as will be shown later.

The amount of air bypassing the PE depends on the temperature required in front of the turbine T_{t45}, which is also denoted as the Ljungström turbine inlet temperature (LTIT).

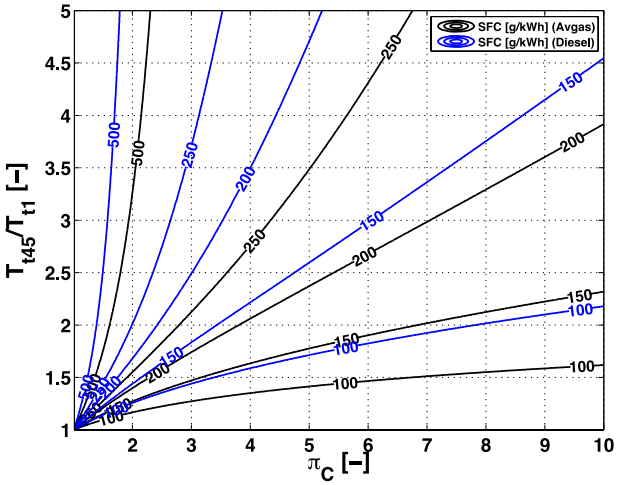

FIG. 7 : PE TDR-CYCLE SFC, AVGAS VS. DIESEL – LOSSLESS COMPRESSOR, LOSSLESS TURBINE, NO TRANSMISSION LOSSES

Defining the bypass ratio BPR as :

(10) $$BPR = \frac{\dot{m}_s}{\dot{m}_p}$$

and substituting Eq.8 in Eq.5, while knowing that $\dot{m} = \dot{m}_p + \dot{m}_s$, it is possible to find after simplification ($\dot{m}_f \ll \dot{m}_t$) :

(11) $$BPR = \frac{\eta_{CC} LHV \cdot FAR}{C_p T_{t1}\left(\frac{C_{pg}}{C_p}\frac{T_{t45}}{T_{t1}} - 1\right)} - 1$$

BPR decreases with an increase in T_{t45}/T_{t1} (Fig. 8). Note that BPR cannot be rendered fully non-dimensional (T_{t1}) and that it is not depending on the compressor pressure ratio π_C. For a given T_{t45}/T_{t1}, BPR will rise with a decrease in inlet temperature T_{t1}. Indeed, under these conditions, if T_{t1} decreases, T_{t45} will drop and $(T_{t45} - T_{t1})$ too. As a consequence, the fraction of exhaust gases on the total mass flow has to be lower, thus BPR will be higher. The temperature of the exhaust gases T_{t4p} depends on BPR, as will be discussed later (Eq.19).

TABLE 1 : FUEL LOWER HEATING VALUES (15°C)

Fuel type	LHV [MJ/kg]	Ref.
Diesel	42.5	[14]
Avgas	43.7	[15]

TABLE 2 : FAR FOR SPI AND DE MAXIMUM CONTINUOUS REGIME [14]

Engine type	ϕ [–]	FAR_{st} [–]	FAR [–]
SPI (Avgas)	1.5	1:14.7	1:9.8
DE (diesel)	0.7	1:14.5	1:20.7

Finally, Fig. 8 clearly shows that DEs have a lower BPR than SPI because of the former's lower ϕ, leading to a higher primary airflow rate requirement.

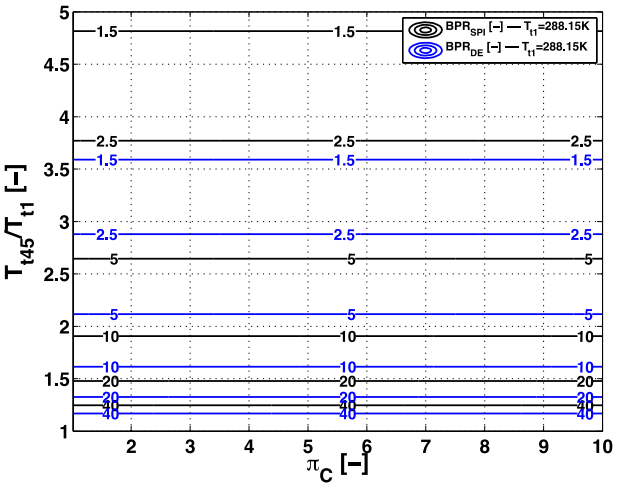

FIG. 8 : PE TDR-CYCLE BPR, AVGAS VS. DIESEL – LOSSLESS COMPRESSOR, LOSSLESS TURBINE, NO TRANSMISSION LOSSES

P_T^* is not necessarily identical to P_M^* since there is no mechanical connection between the PE and the RELT. The PE only delivers a mechanical power P_M^* to the compressor absorbing a power P_C^*, where :

(12) $$P_C^* = \eta_M P_M^*$$

and η_M the mechanical efficiency for the transmission system between PE and compressor drive shaft. The difference between P_T^* and P_M^* can be expressed by the definition of a cycle coefficient of performance COP:

(13) $$COP = \frac{P_T^*}{P_M^*}$$

Substitution of Eq.4 and Eq.12 in Eq.13 and assuming that $\dot{m}_t \cong \dot{m}$ yields for COP :

(14) $$COP = \eta_M \frac{C_{pg}}{C_p} \frac{T_{t45}}{T_{t1}} f_{COP}(\pi_C)$$

where,

(15) $$f_{COP}(\pi_C) = \frac{1 - \left(\frac{1}{\pi_C}\right)^{\frac{\gamma_g - 1}{\gamma_g}\eta_{p,T}}}{\pi_C^{\frac{\gamma-1}{\gamma}\frac{1}{\eta_{p,C}}} - 1}$$

The variable $\eta_{p,C}$ is the compressor polytropic efficiency. For given polytropic efficiencies, Eq.14 and Eq.15 clearly show that an increase in T_{t45}/T_{t1} and decrease in π_C are beneficial (Fig. 9). As a matter of fact, increasing LTIT increases the specific power output of the turbine. However, the beneficial effect of an increasing π_C on the turbine power output is undone by the rise in specific power demand of the compressor, as revealed by the f_{COP} parameter. Eq.14 shows that it is possible that $COP \lessgtr 1$. For conventional helicopters, the power delivered to the rotors is always lower than the power delivered by the engine because of the inevitable transmission losses. The TDR concept now shows *the potential* to have a COP higher than unity, where the turbine delivers more power to the rotors than what is delivered by the engine, thanks to recycling of the exhaust gases in the RELT.

Finally note that on Fig. 9 COP of a DE is slightly higher than COP of a SPI. The cause lies with the simplified calculation of C_{pg}, which is little higher for diesel fuel.

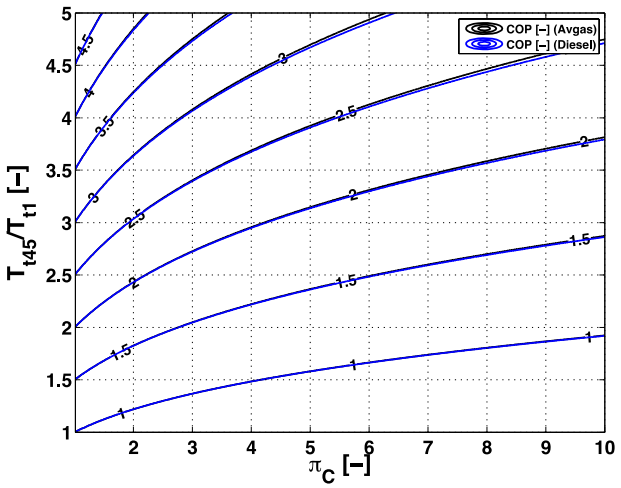

FIG. 9 : PE TDR-CYCLE COP, AVGAS VS. DIESEL – LOSSLESS COMPRESSOR, LOSSLESS TURBINE, NO TRANSMISSION LOSSES

3.2.2 **Cycle boundary conditions**

Before studying the results of the cycle, it is important to define the physical operating boundaries of the cycle.

Firstly, the Carnot efficiency ϵ_{Carnot} must be considered, where

(16) $$\epsilon_{Carnot} = 1 - \frac{T_L}{T_H}$$

T_H is the temperature of the hot heat source in the cycle. For this purpose, the adiabatic flame temperature could be used, which is around 2500K[15]. T_L is the temperature of the cold heat source, i.e. the surroundings at ambient temperature T_{t1}.

Even though the Carnot efficiency only applies to closed cycles, it is conceivable to close the cycle fictitiously and add imaginary heat exchangers. Here, the effects of the combustion process are tacitly disregarded seeing that the fuel mass flow is usually much smaller than the mass flow of air. The thermal efficiency of the cycle ϵ_{th} should always be less or equal to ϵ_{Carnot}.

Secondly, the temperature of the exhaust gases of the PE should always be higher than the gases entering the PE, i.e.

(17) $$T_{t4p} \geq T_{t2p}$$

Since the PE needs proper cooling, a fraction x_c of the heat released by the combustion process is absorbed by the secondary flow. This is represented in Fig. 6 by the parameter Q_c. x_c usually amounts to about 35%[13] of the total heat input.
T_{t2p} may be found via the simple thermodynamic relation for adiabatic compression :

$$T_{t2p} = T_{t2} = T_{t1}\pi_C^{\frac{\gamma-1}{\gamma}\frac{1}{\eta_{p,C}}} \tag{18}$$

Application of the first law on CV2 (Fig. 6), then delivers for the exhaust gas temperature :

$$T_{t4p} = \frac{C_p}{C_{pg}}T_{t1}\left[\pi_C^{\frac{\gamma-1}{\gamma}\frac{1}{\eta_{p,C}}}\left(1-\frac{1+BPR}{\eta_M}\right)+\ldots \frac{1+BPR}{\eta_M}\right]+\frac{(1-x_c)\eta_{CC}LHV\cdot FAR}{C_{pg}} \tag{19}$$

If $T_{t4p} = T_{t2p}$, the limiting pressure ratio $\pi_{C_{BD}}$ is found :

$$\pi_{C_{BD}} \leq \left[\frac{\frac{1+BPR}{\eta_M}\frac{C_p}{C_{pg}}+\frac{(1-x_c)\eta_{CC}LHV\cdot FAR}{C_{pg}T_{t1}}}{\frac{1+BPR}{\eta_M}\frac{C_p}{C_{pg}}+1-\frac{C_p}{C_{pg}}}\right]^{\frac{\eta_{p,C}\cdot\gamma}{\gamma-1}} \tag{20}$$

Thirdly, the PE specific fuel consumption SFC_{PE} range has to be imposed. During the development of the previous equations, no attention was given to the operating characteristics of the PE itself. PEs work within a well established SFC_{PE} range (Table 3).
Note that for a given T_{t1} and PE type, selecting SFC_{PE} and a compression ratio π_C determines the operating point in the cycle. Indeed, for a given fuel flow rate $\dot{m}_f$, SFC_{PE} and η_M, the power delivered to the compressor P_C^* can be found. From Eq.34, $\dot{m}$ can be obtained. This allows the retrieval of T_{t45}/T_{t1}, BPR and COP. At this point, it is also interesting to express the relation between COP and SFC for a given SFC_{PE}. It is easily proven that :

$$COP = \frac{SFC_{PE}}{SFC} \tag{21}$$

COP could therefore also be regarded as the cycle relative specific fuel consumption, or how good the cycle specific fuel consumption is with respect to the one of the PE.

TABLE 3 : PE SPECIFIC FUEL CONSUMPTION DATA [14] AND MARKET SURVEY PERFORMED BY THE AUTHORS

Type	intake†	strokes	SFC_{PE} [g/kWh]
SPI Avgas	atm.	4	250…400
SPI Avgas	turbo	4	250…400
SPI E95	atm.	2	350…600
Diesel	turbo	4	220…320
Diesel	turbo	2	220…320

† Conditioning of air near intake manifold : atm. = atmospherically aspirated
turbo = turbocharger

3.2.3 **Pre-compression**
Because the PE is installed in the pressurised environment (plenum – Fig. 5), the PE delivers a higher power output. The power output of a PE is indeed proportional to air density[13]. The available power P_M^* will hence depend on the compression ratio π_C. Defining $P_{M,a}^*$ as the installed power under atmospheric conditions, P_M^* then is :

$$P_M^* = \frac{\rho_{t2}}{\rho_{ta}}P_{M,a}^* \tag{22}$$

Designating an inlet loss factor RR to account for the total pressure losses in the inlet of the plenum and compressor, viz. :

$$RR \triangleq \frac{p_{t1}}{p_{ta}} \tag{23}$$

it is possible for an adiabatic inlet to rewrite Eq.22 as :

$$P_M^* = PCF \cdot P_{M,a}^* \tag{24}$$

where PCF is defined as the pre-compression factor, i.e. :

$$PCF \triangleq RR \cdot \pi_C^{\frac{1-\gamma}{\gamma}\frac{1}{\eta_{p,C}}+1} \tag{25}$$

It is important to note that increasing PCF will result in higher PE inlet temperatures T_{t2p}. However, it does not necessarily limit the PE operational domain. As long as PCF is not too high, the cylinder head temperature may remain well within specifications, as the combustion process is intermittent, thus less susceptible to the higher combustion temperatures. Nevertheless, good temperature monitoring will be indispensable and will undoubtedly impose boundaries on the maximum value of π_C. Also note that the effect of pre-compression on PEs with supercharging needs further analysis (impact on turbocharger operations) and that the crankshaft must withstand the higher torque delivered by the engine.
As a result of the pre-compression, a smaller and consequently lighter PE can be installed. Even though delivering a power P_M^*, the PE was however intended to produce a lower power $P_{M,a}^*$ under atmospheric conditions, without precompression. As a result, pre-compression has a beneficial impact on the helicopter propulsion system weight. Since conventional helicopter engines are not using pre-compression, it is interesting to define an equivalent coefficient of performance $ECOP$ where the installed power under atmospheric conditions is compared to the delivered power by the RELT :

$$ECOP \triangleq \frac{P_T^*}{P_{M,a}^*} = PCF \cdot COP \tag{26}$$

Hence, $ECOP$ should be taken into account when assessed against the mechanical transmission

efficiency of a conventional helicopter or COP, in case of other non-pre-compressed (TDR) cycles.

3.2.4 **Avgas SPI PE example and discussion**

The theory expounded in the previous sections is now applied on a SPI PE, introducing realistic values for the cycle component efficiencies (Table 4). Only ISA SLS conditions will be examined. For the compressor, a single-stage or multi-stage centrifugal compressor is considered. Indeed, for the lower mass flows it exhibits better weight, dimension and performance characteristics than the axial compressor[10]. When a higher mass flow is required, another cycle will become more interesting, as will be discussed later in this paper (turbofan). Note that the used polytropic efficiency of the compressor is rather high, but if it is tailor-made compressor, it is acceptable[17]. As a matter of fact, the subsequent performance discussion will prove that high pressure ratios are not recommended for the actual TDR configurations, being subjected to a low T_{t45}/T_{t1} limit. This again, endorses the use of a high compressor efficiency.

The performance evaluation of the SPI PE cycle may now be performed by analysing Fig. 10.

The performance characteristics of the cycle depend on the non-dimensional LTIT (T_{t45}/T_{t1}) and the compressor pressure ratio π_C. In addition, the usable SFC_{PE} range (gray lines) further defines the usable domain. Indeed, the relevant type of PE exhibits typical SFC_{PE} characteristics (Table 3), which are reasonably independent of density changes and thus π_C [13]. Further limitations are the cycle boundary conditions, of which the most stringent is plotted in Fig. 10, viz. $\pi_{C_{BD}}$ (red line). In case grease lubricated bearings are used, the maximum RELT operating temperature should be not higher than 400K (as indicated in several bearing catalogues). Hence, a T_{t45}/T_{t1} -limit should also be respected for given atmospheric conditions. This limit is indicated by a red dashed line. This further reduces the useful operating domain of the cycle. Taking the aforementioned cycle boundaries into account, the pressure ratio ranges no higher than about 2, which approves the use of a high compressor efficiency.

For a given PE and thus SFC_{PE}, maximum power output, i.e. high COP and $ECOP$, is found with high T_{t45}/T_{t1} settings. This concurs also with an increase in π_C because the PE needs a higher inlet temperature to attain the required LTIT. This also explains why the more efficient engine has to operate at higher π_C.
Note that the effect of increasing π_C has a negative impact on COP due to f_{COP}, as described earlier. The less efficient SPI therefore has a better COP than the more efficient PE. The preferred engine will consequently depend on the mission profile, where a tradeoff between fuel weight and empty weight will have to be performed, but it would not be unsensible to sacrifice COP and thus cycle efficiency to reduce the mission fuel weight.

Depending on the efficiency of the selected SPI, a COP between 90-95% is possible. As a consequence, SFC will be 5%-10% higher, but this could be justified by the reduced gross weight of the helicopter since the heavy transmission system is no longer present, accounting for approximately 20%[18]* of the helicopter gross weight, the 4-9% engine power loss in the transmission system[25], the 5-10% of power consumed by the tail rotor[26], and the minor weight benefits thanks to pre-compression. Interestingly, when working at maximum T_{t45}/T_{t1}, $ECOP$ is significantly larger than unity.
In case the T_{t45}/T_{t1} -limit would be increased, COP could be higher than unity, but this would require other RELT materials and cooling of the rotor head bearings, which will only make the system more complex and heavier. This should be assessed against the weight sacrifices. At this point the authors believe that the best way to improve COP is to improve the turbine polytropic efficiency.

TABLE 4 : SPI PE CASE STUDY

Variable		note
η_{CC} [-]	0.67	Eq.6
η_M [-]	0.98	simple GBX
RR [-]	1.00	lossless inlet
$\eta_{p,C}$ [-]	0.90	[17]
$\eta_{p,T}$ [-]	0.85	[5]$^{\Delta}$
γ … γ_g [-]	1.4 … 1.33	[16]
R_g [J/kgK]	287.05	[10]
T_{t45}/T_{t1} limit [-]	1.39	GLB

† GLB : grease lubricated bearings. Maximum operating temperature 400K

Δ Prospective efficiency estimation based on Ljungström turbine study in [5]

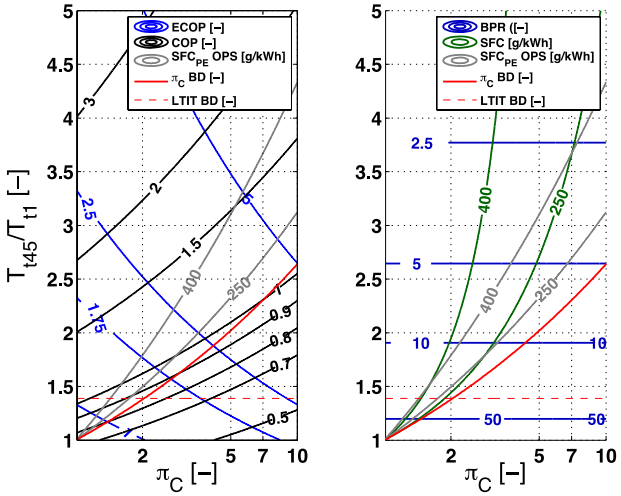

FIG. 10 : SPI TDR-CYCLE PERFORMANCE CHART, ISA SLS (SEE ALSO TABLE 4)

* Note that the RELT will increase the weight of other components, such as the rotor head, but this is expected to be negligible with respect to the weight of the transmission system of the conventional helicopter.

3.2.5 **Diesel PE example and discussion**

The cycle parameters using the DE are reflected in Table 5. The same boundary conditions are in effect as explained for the SPI in the previous section. The major difference here is the reduced $SFC_{(PE)}$, the narrower SFC_{PE} operating domain, and the lower BPR because of the much lower ϕ (Fig. 11) and the slightly lower LHV (Table 1).

The optimum operating conditions may again be found with the higher T_{t45}/T_{t1}, where at the T_{t45}/T_{t1}-limit, COP is between 91% and 96%, which is a bit higher than what is observed with the SPI. Similar conclusions may be drawn as done with the SPI.

TABLE 5 : DE PE CASE STUDY

Variable		note
η_{CC} [-]	0.99	low ϕ
η_M [-]	0.98	simple GBX
RR [-]	1.00	lossless inlet
$\eta_{p,C}$ [-]	0.90	[17]
$\eta_{p,T}$ [-]	0.85	[5]$^{\Delta}$
γ ... γ_g [-]	1.4 … 1.33	[16]
R_g [J/kgK]	287.05	[10]
T_{t45}/T_{t1} limit [-]	1.39	GLB

† GLB : grease lubricated bearings. Maximum operating temperature 400K

Δ Prospective efficiency estimation based on Ljungström turbine study in [5]

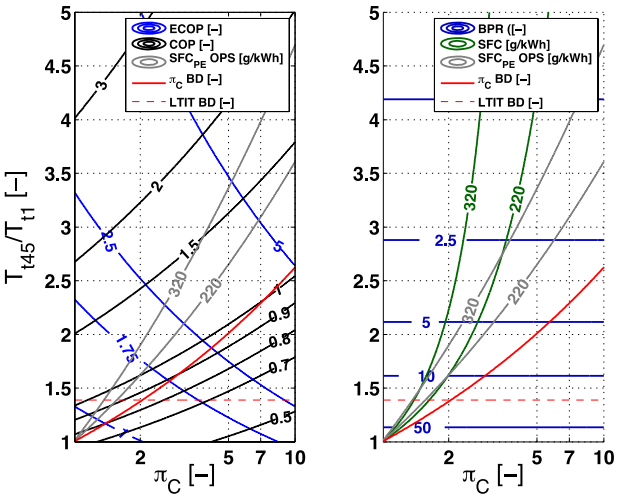

FIG. 11 : DE TDR-CYCLE PERFORMANCE CHART, ISA SLS (SEE ALSO TABLE 4)

3.2.6 **SPI vs. DE**

From the previous evaluations, it was established that the DE performed slightly better than SPI (higher COP and lower SFC). However, the performance charts did not expound the effect of weight between both engine types. Indeed, if the DE requires a lower π_C, PCF is lower and for the same P_T^*, $P_{M,a}^*$ must be higher and so will be $\dot{m}_f$. Further thermodynamic examination of the cycles, which will not be discussed in this work, imposing equal P_T^*, shows that for a given T_{t45}/T_{t1} and SFC_{PE} , the DE will always consume less fuel in absolute terms. Though, $ECOP$ of the DE will lower, thus requiring a heavier engine. Again, the choice whether to select an SPI or DE, will depend on the mission profile of the helicopter.

3.3 **The Turboshaft Engine TDR-Cycle**

3.3.1 **Cycle performance parameter definition**

The turboshaft engine (TS) is known for its superior power-to-weight ratio with respect to the PE for the higher power demands. The TS is frequently used in conventional helicopters and it is therefore interesting to examine whether this engine could be used for the TDR-helicopter.

The general cycle requires recovering as much heat as possible from the ICE in order to be efficient. TS are not as robust as PE and are designed to operate under atmospheric conditions. Indeed, high PCF are not recommended, neither from a pressure nor a temperature viewpoint. As a consequence, it is not sensible to install the TS in the plenum. Otherwise, important design modifications will be required to the off-the-shelf engine, which is at this point not economically justified. In order to cope with that issue, a heat exchanger (HEX) is introduced in the cycle, which is demonstrated in Fig. 12.

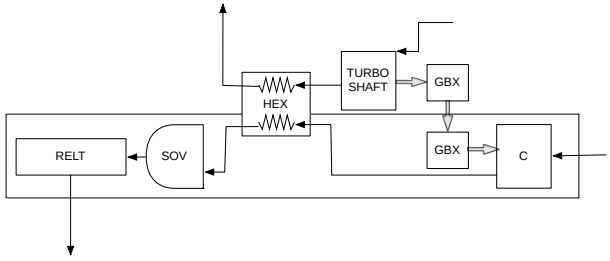

FIG. 12 : THE TURBOSHAFT ENGINE TDR-CYCLE

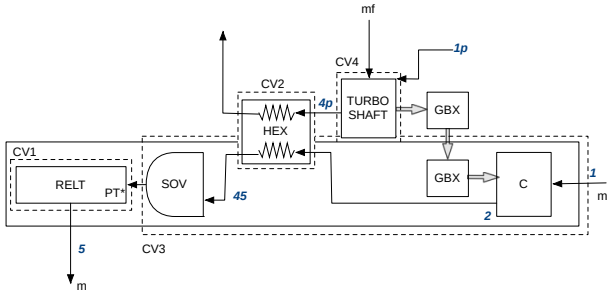

FIG. 13 : THE TURBOSHAFT ENGINE TDR-CYCLE BREAKDOWN

The cycle layout is similar to the one established for the PE, but differs from it by putting the TS outside the plenum. As a result of this, it is plausible that the output shaft of the TS will have to be connected to the compressor via a small transmission system. Note that only pure air is going through the RELT. Hence, the beneficial impact of the higher heat capacity of the exhaust gas mixture on the RELT power output is lost.

Executing the cycle study using Fig. 13 on a similar basis as seen with the PE, allows establishing formulae for the performance parameters. The development of these formulae is not included in this work.

For the TS-cycle, the power delivered by the RELT is :

$$P_T^* = \dot{m} C_p T_{t45} \left[1 - \left(\frac{1}{\pi_C} \right)^{\frac{\gamma-1}{\gamma}\eta_{p,T}} \right] \tag{27}$$

Note that no exhaust gases go through the RELT. This mass flow is consequently lost. This will inevitably lead to a lower cycle efficiency (see the general cycle discussion).

If the power delivered by the TS is P_M^*, the cycle specific fuel consumption SFC becomes :

$$SFC = \frac{SFC_{TS} P_M^*}{\dot{m} C_p T_{t45} \left[1 - \left(\frac{1}{\pi_C} \right)^{\frac{\gamma-1}{\gamma}\eta_{p,T}} \right]} \tag{28}$$

where SFC_{TS} is defined as the specific fuel consumption of the TS. SFC_{TS} depends on the power class of the TS. The more powerful the TS, the lower SFC_{TS} becomes. Eq.28 can be further developed to find :

$$SFC = \frac{SFC_{TS}}{\eta_M \; f_{COP}(\pi_C) \; \frac{T_{t45}}{T_{t1}}} \tag{29}$$

SFC is proportional to SFC_{TS} and is affected by the mechanical losses η_M in the interconnecting transmission system. The other non-dimensional parameters were already found in the PE study. $f_{COP}(\pi_C)$ is a decreasing function of π_C, so a rise in π_C and/or a drop in T_{t45}/T_{t1} increases the SFC. Indeed, the increased power production of the RELT is again outweighed by the increased power demand of the compressor ($f_{COP}(\pi_C)$-parameter), while the drop in T_{t45}/T_{t1} means less heat was recuperated for a given SFC_{TS}.

COP is again found to be a figure of merit for the cycle relative specific fuel consumption (Eq.21) :

$$COP = \frac{SFC_{TS}}{SFC} \tag{30}$$

Eq.29 also shows :

$$COP = \eta_M \frac{T_{t45}}{T_{t1}} f_{COP}(\pi_C) \tag{31}$$

Eq.31 is identical to Eq.14, but the heat constant ratio drops out the equation since only air passes through the RELT. The behaviour of COP is thus similar to the PE cycle, i.e. a high T_{t45}/T_{t1} and low π_C are beneficial. Note that since the TS is not installed in the plenum (Fig. 12), $PCF = 1$ and consequently : $ECOP = COP$.

A bypass ratio BPR for the TS cycle may also be defined :

$$BPR = \frac{\dot{m}}{\dot{m}_p} \tag{32}$$

where $\dot{m}_p$ the air passing through the TS and $\dot{m}$, the air entering the RELT. BPR is then found to be :

$$BPR = \frac{\eta_M FAR}{SFC_{TS} C_p T_{t1} (\pi_C^{\frac{\gamma-1}{\gamma}\frac{1}{\eta_{p,C}}} - 1)} \tag{33}$$

BPR increases when π_C decreases. Then indeed, the compressor converts most of the power delivered by the TS to mass flow $\dot{m}$:

$$\dot{m} = \frac{\eta_M P_M^*}{C_p T_{t1} (\pi_C^{\frac{\gamma-1}{\gamma}\frac{1}{\eta_{p,C}}} - 1)} \tag{34}$$

Also, when FAR is low, BPR will be low because the TS must ingest more air to deliver its power. Note that in contrast to the PE-cycle, BPR is not a function of T_{t45}/T_{t1}, but of π_C instead.

Finally, it is important to define the HEX efficiency ϵ_H, which is[19] :

$$\epsilon_H = \frac{\dot{Q}_{ex}}{\dot{Q}_{\Delta T_{max}}} \tag{35}$$

and,

$$\dot{Q}_{ex} = \dot{m} C_p (T_{t45} - T_{t2}) \tag{36}$$

$$\dot{Q}_{\Delta T_{max}} = min\left\{ \dot{m}_p C_{pg} (T_{t4p} - T_{t2}); \dot{m} C_p (T_{t4p} - T_{t2}) \right\} \tag{37}$$

3.3.2 **Cycle boundary conditions**

Before exploring the performance characteristics in detail, it is important to set the cycle boundary conditions.

For heat to be exchanged to the bypass flow, $T_{t4p} \geq T_{t2}$. This sets a maximum to π_C, viz. $\pi_{C,L1}$:

$$\pi_C \leq \left[\frac{C_p}{C_{pg}} + \frac{FAR}{T_{t1} C_{pg}} \left(\eta_{CC} LHV - \frac{1}{SFC_{TS}} \right) \right]^{\frac{\eta_{p,C} \cdot \gamma}{\gamma - 1}} \triangleq \pi_{C,L1} \tag{38}$$

In addition, the heat exchange process must obey thermodynamic equilibrium limitations :

$$\dot{Q}_{ex} \leq \dot{Q}_{\Delta T_{max}} \tag{39}$$

$\dot{Q}_{\Delta T_{max}}$ may be found via BPR, retrieving a critical value for BPR, defined as BPR_{L2} :

(40)
$$BPR \leq \frac{C_{pg}}{C_p} \triangleq BPR_{L2} \quad \Rightarrow \quad \dot{Q}_{\Delta T_{max}} = \dot{m} C_p (T_{t4p} - T_{t2})$$
$$BPR > \frac{C_{pg}}{C_p} \triangleq BPR_{L2} \quad \Rightarrow \quad \dot{Q}_{\Delta T_{max}} = \dot{m}_p C_{pg} (T_{t4p} - T_{t2})$$

This is a second boundary. If $BPR \leq BPR_{L2}$, the caloric capacity of the primary mass flow dominates, resulting in a limit for T_{t45}/T_{t1} :

(41)
$$\frac{T_{t45}}{T_{t1}} \leq \frac{C_p}{C_{pg}} + \frac{FAR}{C_{pg} T_{t1}} \left(\eta_{CC} LHV - \frac{1}{SFC_{TS}} \right) \triangleq \left[\frac{T_{t45}}{T_{t1}} \right]_{L2,1}$$

This limit is independent of π_C. For the condition $BPR > BPR_{L2}$, the caloric capacity of the secondary mass flow dominates, which imposes $T_{t45} < T_{t4p}$. The limit for T_{t45}/T_{t1} then becomes :

(42)
$$\frac{T_{t45}}{T_{t1}} \leq \left(1 - \frac{C_{pg}}{C_p} \frac{1}{BPR} \right) \pi_C^{\frac{\gamma - 1}{\gamma \eta_{p,C}}} + \frac{1}{BPR} \left[1 + \ldots \right.$$
$$\left. \frac{FAR}{C_p T_{t1}} \left(\eta_{CC} LHV - \frac{1}{SFC_{TS}} \right) \right] = \left[\frac{T_{t45}}{T_{t1}} \right]_{L2,2}$$

This limit is depending on π_C via BPR. The transition between both caloric regimes in Eq. 40 occurs at $\pi_{C,L2}$:

(43)
$$\pi_C \leq \left(\frac{\eta_M FAR}{SFC_{TS} T_{t1} C_{pg}} + 1 \right)^{\frac{\gamma \eta_{p,C}}{\gamma - 1}} \triangleq \pi_{C,L2}$$

The third boundary imposes that $T_{t45} \geq T_{t2}$, hence a third limit is imposed on π_C, viz. $\pi_{C,L3}$:

(44)
$$\pi_C \leq \left(\frac{T_{t45}}{T_{t1}} \right)^{\frac{\gamma \eta_{p,C}}{\gamma - 1}} \triangleq \pi_{C,L3}$$

The final boundary comes from the cycle Carnot efficiency, which then yields $T_{t4p} \geq T_{t1}$.

Finally, note that an estimation of T_{t4p} follows from CV4 in Fig. 13, giving :

(45)
$$T_{t4p} = \frac{C_p}{C_{pg}} T_{t1} + \frac{FAR}{C_{pg}} \left(\eta_{CC} LHV - \frac{1}{SFC_{TS}} \right)$$

Values for FAR and LHV may be found in Table 6.

TABLE 6 : TURBOSHAFT PERFORMANCE CHARACTERISTICS

Variable		Ref.
LHV Kerosene [MJ/kg]	43.2	[20]
FAR [-]	1:60	[21]
SFC_{TS} [g/kWh]	280…479	Survey

3.3.3 **Example and discussion**

Table 7 summarises the cycle parameters used in the TS TDR-cycle study. Only ISA SLS conditions are again studied. The performance characteristics of the cycle will be examined parametrically, using T_{t45}/T_{t1}, π_C and the heat exchanger efficiency ϵ_H as independent variables. Also, SFC_{TS} is an independent variable, but the concurring results will be plotted separately in order to enhance readability.

Fig. 14 and Fig. 15 reflect the results of the parametric study. The black lines on the graphs are the aforementioned cycle boundaries. The operating range is within the triangular shaped domain, wherein the HEX ϵ_H lines are plotted (red lines). This domain is further restrained by the LTIT temperature boundary, revealed on the plot by the dashed red line.

TABLE 7 : TS CASE STUDY

Variable		note
η_{CC} [-]	0.99	[21]
η_M [-]	0.98	simple GBX
$\eta_{p,C}$ [-]	0.90	[17]
$\eta_{p,T}$ [-]	0.85	[5]$^{\Delta}$
γ … γ_g [-]	1.4 … 1.33	[21]
R_g [J/kgK]	287.05	[10]
T_{t45}/T_{t1} limit [-]	1.39	GLB
SFC_{TS} [g/kWh]	280-479*	survey

† GLB : grease lubricated bearings. Maximum operating temperature 400K

Δ Prospective efficiency estimation based on Ljungström turbine study in [5]

* Concurs with a shaft power output of resp. 2 MW – 100 kW

To be competitive with the conventional helicopter, COP near unity shoud be strived for (Fig. 14). As a result of the LTIT limit, rather high ϵ_H are therefore necessary. For the high power class TS exhibiting the lowest SFC_{TS}, this requirement is even more important. Indeed, the more efficient the engine is, the lower its exhaust gas temperature, so a more efficient HEX is then essential to achieve same T_{t45}/T_{t1} levels. A direct consequence of this is also the lower maximum achievable value of T_{t45}/T_{t1}. For the small power class TS (100 kW-range - Table 7), where $SFC_{TS} > SFC_{PE}$, $COP$is found to be close to unity for moderate and high ϵ_H (0.6-0.8), and SFC will consequently be a little higher than SFC_{TS}. However, this comes at an important fuel cost ($SFC_{TS} > SFC_{PE}$). For the high power class TS on the other hand, with $SFC_{TS} \cong SFC_{PE}$, COP is around 90%, which is not very attractive compared to what is achievable with the PE-cycle.

Note that because of the low LTIT boundary, again it appears that a low pressure ratio is required for the cycle, which substantiates the choice of $\eta_{p,C}$.

Fig. 15 reflects the BPR of the cycle. It is interesting to note that BPR of TS is much lower than the one observed with PE. The reason is found with the significantly lower FAR of the TS. BPR increases clearly when SFC_{TS} decreases, because the more efficient engine produces more power and consequently delivers more mass flow for a given π_C.

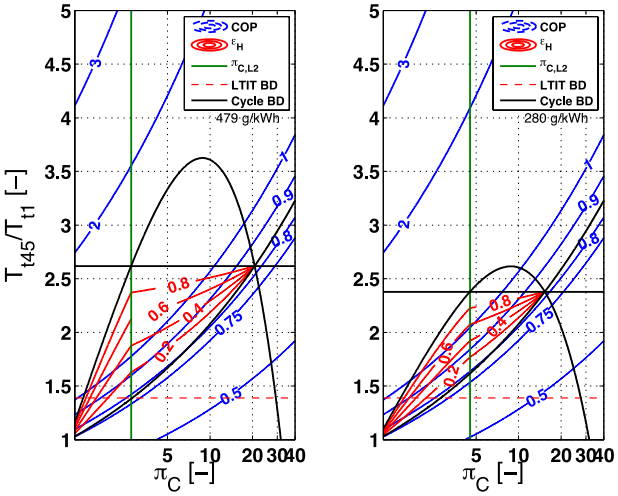

FIG. 14 : TS TDR-CYCLE PERFORMANCE CHART, ISA SLS COP (SEE ALSO TABLE 7)

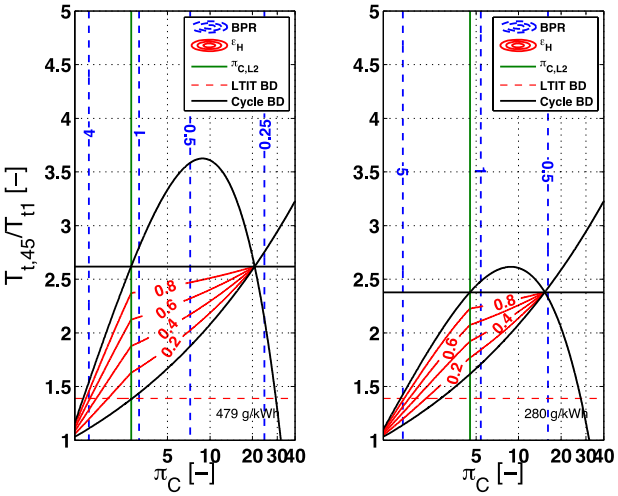

FIG. 15 : TS TDR-CYCLE PERFORMANCE CHART, ISA SLS BYPASS RATIO (SEE ALSO TABLE 7)

3.3.4 **Cycle drawbacks**

Even though the proposed TS-cycle appears promising, it is quite misleading. First of all the mass of the HEX needs serious consideration. The work of Semple[22] reflects the impact of ϵ_H on the HEX mass per unit of mass flow rate (Fig. 16). The weight trend was established for a shell-and-tube recuperator installed in a TS with $BPR = 1$. Of concern is that the TS-cycle $BPR \cong 5$, will increase the weight fraction proportionaly. Especially when an efficient TS is installed, the detremental impact will be the highest. Regenerators might be a lighter and more efficient option, but they are not mature for implementation and cause a higher system complexity[23].

Secondly and most importantly, the TS-cycle is inferior to the PE-cycle for the low power class SFC_{TS}, and thanks to the pre-compression, likely also for the mid power class. For the high power class TS, HEX weight appears to become an issue. Hence, a third cycle is proposed, using a turbofan.

Thirdly, since no off-the-shelf (OTS) TS-solution is expected to be available resulting in the need of a HEX, because the increased complexity of the system and due to the negative weight impact, the TS-cycle is, at this point, not recommended to be implemented in the TDR-helicopter.

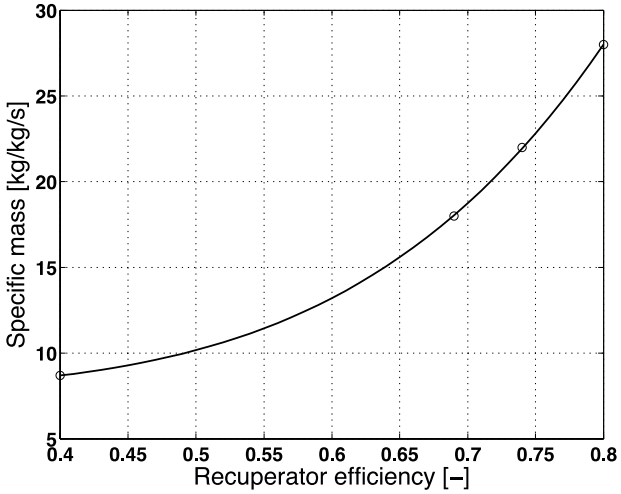

FIG. 16 : TS HEX MASS CONSIDERATIONS, SHELL-AND-TUBE, BPR=1, FIGURE REPLOTTED FROM [22]

3.4 **The Turbofan Engine TDR-Cycle**

From the previous analysis, low pressure ratio and temperature operating points emerged as the recommended operating points. Although the main purpose of the turbofan (TF) is to provide thrust, the exhaust is highly energetic. It is consequently sensible to examine the potential of this engine in a TDR-cycle. Note that the TDR-helicopter may benefit from the thrust capability of the TF, alleviating the rotors and enabling an extended flight envelope.

The TF TDR-cycle is represented in Fig. 17. Note that more than one TF may be installed.

3.4.1 **Cycle performance parameters**

The performance characteristics of the cycle may again be retrieved by examination of the CVs indicated in Fig. 18. However, the definition of COP will no longer be on the same basis, since the TF is not producing any mechanical power P_M^*. The performed parametric study will be limited to two important TF design characteristics : the TF bypass ratio BPR_{TF}, which is the ratio of secondary and primary air flows, and the fan total pressure ratio π_F. Considering the total pressure losses in the bypass nozzle to be negligible and assuming the total pressure difference between the exhaust gases leaving the core of the engine and the secondary flow to be negligible, it is reasonable to state that :

(46) $$\pi_T = \pi_F$$

and consequently :

(47) $$P_T^* = \dot{m}_t C_{pg} T_{t45} \left[1 - \left(\frac{1}{\pi_F} \right)^{\frac{(\gamma_g - 1)}{\gamma_g} \eta_{p,T}} \right]$$

Note that the mixing of bypass and core mass flows is considered to be completed before entering the RELT. As mentioned before, the TF may be used to provide propulsive force to the helicopter platform, requiring an amount of high-energy air to be bled off. Defining the thrust factor τ_f as :

(48) $$\tau_f = \frac{T_P}{T_{Nt}} \approxeq \frac{\dot{m}_{TF}}{\dot{m}}$$

where T_P the provided propulsive thrust to the helicopter platform, T_{Nt} the total installed thrust of all TFs and $\dot{m}_{TF}$ the mass flow bled from the cycle to produce thrust. Eq.47 may be rewritten as :

(49) $$P_T^* = \frac{(1 - \tau_f) T_{Nt}}{SPT} C_{pg} \frac{T_{t45}}{T_{t1}} T_{t1} \left[1 - \left(\frac{1}{\pi_F} \right)^{\frac{(\gamma_g - 1)}{\gamma_g} \eta_{p,T}} \right]$$

The used fuel mass flow is derived from the TF thrust specific fuel consumption $TSFC$, which is for a number of engines N_e :

(50) $$\dot{m}_f = N_e \cdot TSFC \cdot T_N = TSFC \cdot T_{Nt}$$

T_N is the thrust of a single TF. Applying the first law on CV2 (Fig. 18), it is possible to find for the temperature fraction T_{t45}/T_{t1} :

(51) $$\frac{T_{t45}}{T_{t1}} = \frac{C_p}{C_{pg}} + \frac{FAR/T_{t1}}{C_{pg}(1 + BPR_{TF})} LHV \eta_{CC}$$

Clearly, T_{t45}/T_{t1} is a decreasing function of BPR_{TF} only. The other parameters are considered to be constant and their definition in Eq.51 is identical to those seen in the previous sections (not repeated here). The decreasing tendency is logic since more secondary flow is mixed with the core exhaust gases, resulting in a lower LTIT.

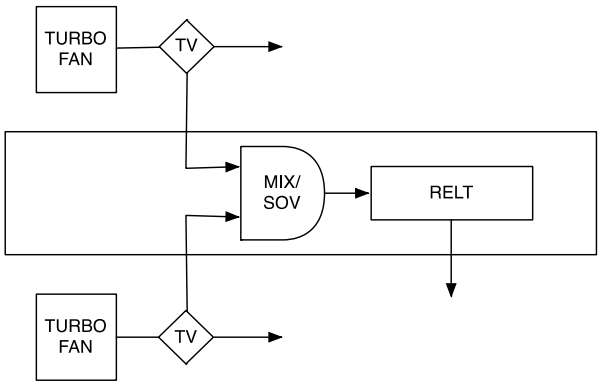

FIG. 17 : THE TURBOFAN ENGINE TDR-CYCLE

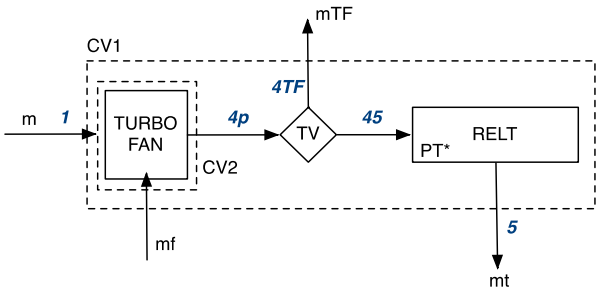

FIG. 18 : THE TURBOFAN ENGINE TDR-CYCLE BREAKDOWN

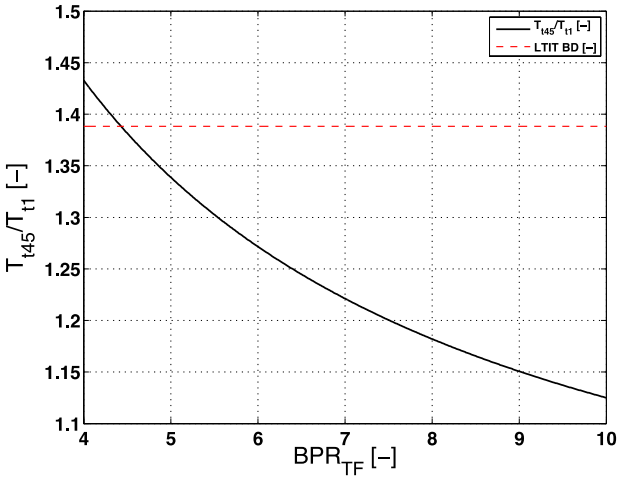

FIG. 19 : LTIT DEPENDENCE ON TURBOFAN BPR

Fig. 19 reveals that most of the T_{t45}/T_{t1} values are well within the usable range of a rotor head with grease-based bearings. Substitution of Eq.51 in Eq.49 yields for P_T^* :

(52) $$P_T^* = \frac{(1 - \tau_f) T_{Nt}}{SPT/T_{t1}} \left[C_p + \frac{FAR/T_{t1}}{(1 + BPR_{TF})} LHV \eta_{CC} \right] \cdot \ldots \left[1 - \left(\frac{1}{\pi_F} \right)^{\frac{(\gamma_g - 1)}{\gamma_g} \eta_{p,T}} \right]$$

A first non-dimensional performance characteristic for the TF-cycle is defined as the power gain PG, which is :

(53) $$PG \triangleq \frac{P_T^*}{T_{Nt}}$$

PG is easily retrieved in Eq.52. PG reflects the amount of available power on the RELT per unit of produced thrust. A priori, PG should thus be selected as high as possible, which concurs with high BPR_{TF} and high π_F (Fig. 20). The effect of τ_f is to decrease PG proportionally.

A second metric for the the efficiency of the cycle is the coefficient of performance COP, but which is now defined quite differently. Indeed, considering the useful energy delivered by the TF to be the increase of kinetic energy to the gases, it is found that :

(54) $$COP_{TF} \triangleq \frac{P_T^*}{\dot{E}_k} \approx \frac{P_T^*}{\frac{1}{2}T_{Nt} \cdot SPT} = \frac{PG}{\frac{1}{2}SPT}$$

SPT is the specific thrust of the engine. Fig. 21 shows the used correlation for this variable, which was developed by the authors, but not discussed in this work. Even though an approximation, it yields an acceptable estimation for the current conceptual analysis. Fig. 20 indicates that COP is mainly a function of π_F. Considering no propulsive thrust to be delivered ($\tau_f = 0$), COP of more than unity is well within reach.

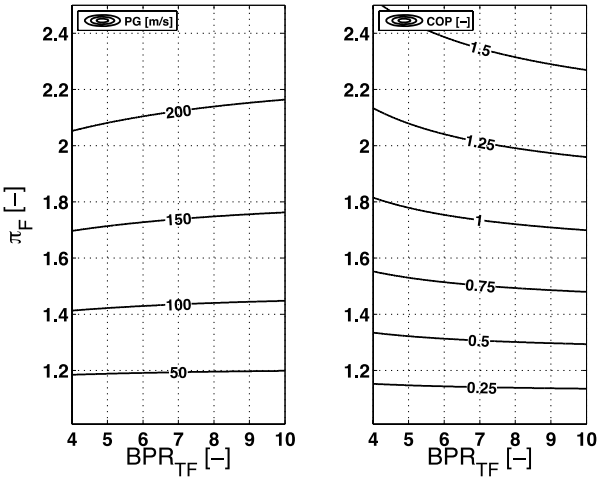

FIG. 20 : PG AND COP AS A FUNCTION OF BPR$_{TF}$, $\tau_F = 0$

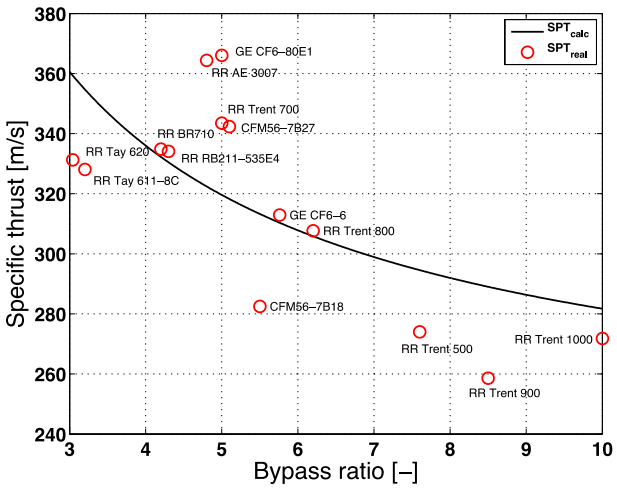

FIG. 21 : TF SPT AS A FUNCTION OF BPR$_{TF}$, TAKE-OFF REGIME ISA SLS

The SFC of the cycle may be found to be :

(55) $$SFC \triangleq \frac{\dot{m}_f}{P_T^*} = \frac{TSFC}{PG}$$

Again, from a survey performed by the authors, an empirical correlation for conceptual purposes has been established (Fig. 22) and was used to plot SFC in Fig. 22. A short discussion of the results is treated next.

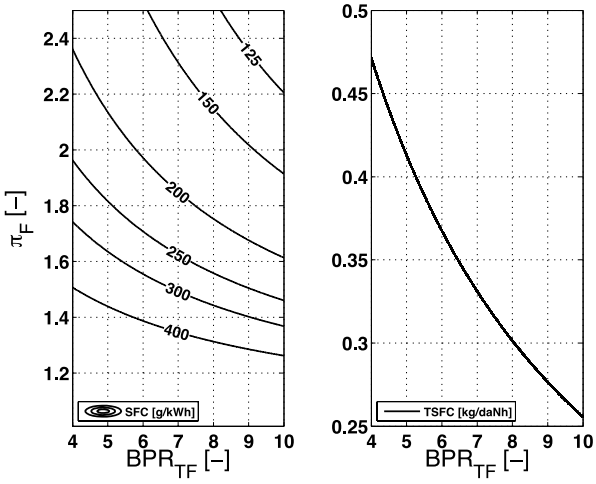

FIG. 22 : TF CYCLE SFC AND TSFC AS A FUNCTION OF BPR$_{TF}$ TAKE-OFF REGIME, ISA SLS

3.4.2 **Example and discussion**

The TF-cycle is now explored using ISA SLS conditions and zero thrust factor. The non-parametrically examined cycle settings are given in Table 8.

Fig. 20 and Fig. 22 clearly expose the potential of the TF-cycle. The higher π_F settings provide the cycle with the higher PG, the higher COP and the lower SFC. If the BPR_{TF} is increased, only PG is minimally sacrificied while T_{t45}/T_{t1} is reduced, which is beneficial for the rotor head bearings. Even though the TF $TSFC$ is given at take-off regime, the TF-cycle clearly shows that it has advantages over the PE-cycle, while it outclasses the TS-cycle. If a feasible π_F is taken of about 1.8[10], SFC may even outperform the SFC_{PE} values of a DE when the BPR_{TF} is high enough. The TF-cycle therefore merits significant attention from the designer, while the PE-cycle will probably be the most cost effective solution for the low power class TDR-helicopter.

Note also that since PG is >100, a small TF may easily deliver high P_T^*, making the TF-cycle available for the mid and high power class helicopters.

TABLE 8 : TF CASE STUDY

Variable		note
η_{CC} [-]	0.99	[21]
$\eta_{p,T}$ [-]	0.85	[5]$^{\Delta}$
γ … γ_g [−]	1.4…1.33	[21]
R_g [J/kgK]	287.05	[10]
T_{t45}/T_{t1} limit [-]	1.39	GLB
LHV Kerosene [MJ/kg]	43.2	[20]
τ_f [-]	0	

† GLB : grease lubricated bearings. Maximum operating temperature 400K

Δ Prospective efficiency estimation based on Ljungström turbine study in [5]

4 CONCLUSIONS

- The TDR-helicopter was introduced and its performance explored thermodynamically using three cycles, each one using a different aero-engine.
- As the RELT is currently limited by a rather low polytropic efficiency, COP is, for the examined cases, always little lower than unity, except for the TF-cycle, where COP *could* be higher. Compared to the losses in the conventional helicopter, the TDR-cycles thus appear sufficiently competitive.
- The TDR-cycles have the potential to reduce the helicopter empty weight because neither a mechanical transmission, nor a tail rotor has to be installed.
- The TF-cycle and the PE-cycle are considered to overlap the operating domain of the TS-cycle. Hence, the latter becomes less attractive from either a weight or a performance viewpoint.
- All cycles operate at low pressure ratios. The PE- and TS-cycles do so because they are restricted by the LTIT limitation of 400K ; the TF-cycle does as well while depending on the fan pressure ratio.
- Only design point performance characteristics were examined.
- A detailed weight study was not performed.

5 PERSPECTIVES

The TDR-helicopter offers a competitive thermodynamic cycle efficiency with respect to conventional helicopters. It allows an extended performance envelope thanks to its coaxial rotor configuration, but also due to its reduced empty weight as the transmission system is no longer required.
The TDR-helicopter off-design characteristics still need to be evaluated meticulously along with the further optimisation of the RELT. TF-cycles are currently examined, while the PE-cycle TDR-helicopter is beign developed by SAGITA (Fig. 23).

FIG. 23 : THE SHERPA TDR-HELICOPTER (LE BOURGET, 2013)

COPYRIGHT STATEMENT

REFERENCES

[1] F. Buysschaert, P. Hendrick, and S. Newman, “Conventional helicopters: an adaptiveness study for more electric and alternative propulsion technologies,” *Journal of Aerospace Engineering*, vol. 226, pp. 1078–1094, 2011.

[2] H. Antoine, G. Dimitriadis, P. Hendrick, E. Kagambage, and T. Rayee, “A novel concept for helicopter rotor drives,” in *3rd European Conference for Aero-Space Sciences*, (Versailles, France), EUCASS, July 6-9 2009.

[3] R. Coppinger, “Helicopter driven by engine exhaust in windtunnel test.” Flight International, 28 July - 3 August 2009.

[4] M. Ramme, “Helicopter rotor and turbine assembly, patent 3417825.” United States Patent Office, 1968.

[5] F. Buysschaert, S. Newman, S. Walker, H. Antoine, and P. Hendrick, “The Ljungström turbine for aeronautical applications,” in *5th European Conference for Aeronautics and Space Sciences*, (München, Germany), EUCASS, July 2013.

[6] W. Runge, F. Buysschaert, J. Hayez, F. Carlier, H. Antoine, P. Hendrick, G. Dimitriadis and G. Degrez, “Numerical and experimental investigation of slot-blowing air over a cylinder,” in *5th European Conference for Aeronautics and Space Sciences*, (München, Germany), EUCASS, July 2013.

[7] F. P. G. Van Loenen Martinet. Mededeelingen betreffende de Ljungstr¨om turbine, vervaardigd door de Svenska Turbinfabriks Aktiebolaget Ljungström te Finspong, Zweden. *De Ingenieur*, 30(30):601–617, July 24th 1915.

[8] A. Houberechts. *les Turbines*. Vander, 1972.

[9] W. W. Peng, *Fundamentals of Turbomachinery*. New Jersey, United States: John Wiley and Sons, Inc., 2008.

[10] P. Walsh and P. Fletcher. *Gas turbine performance*. Blackwell Publishing, 2nd edition, 2004.

[11] C. F. Taylor. *The Internal-Combustion Engine in Theory and Practice, volume 1* : Thermodynamics, Fluid Flow, Performance. The M.I.T. Press, 1985.

[12] J. Leishman. *The Helicopter. Thinking Forward Looking Back*. College Park Press, 2007.

[13] C. F. Taylor. *The Internal-Combustion Engine in Theory and Practice, volume 2* : Combustion, Fuels, Materials, Design. The M.I.T. Press, 1985.

[14] Bosch. *Automotive Handbook*. Robert Bosch GmbH, 7th edition, 2007.

[15] E. Torenbeek and H. Wittenberg. *Flight Physics. Essentials of Aeronautical Disciplines and Technology*, with Historical Notes. Springer, 2009.

[16] N. Cumpsty. *Jet Propulsion : a simple guide to the aerodynamic and thermodynamic design and performance of jet engines*. Cambridge University Press, 2000.

[17] R. Van den Braembussche. *Centrifugal compressors analysis and design*. Von Karman Institute, March 2013.

[18] M. N. Beltramo. Parametric study of helicopter aircraft systems, costs and weights. NASA CR-152315, January 1980.

[19] M. Moran and H. Shapiro. *Fundamentals of Engineering Thermodynamics*. John Wiley and Sons, Inc., 5th edition, 2004.

[20] AIR BP. Handbook of products. Hertfordshire, United Kingdom, 2000.

[21] R. Jacques. *Energetische studie der propulsieturbomotoren. Deel I : theorie*. Vrije Universiteit Brussel, 2004.

[22] R. D. Semple. Research requirements for development of regenerative engines for helicopters. NASA CR-145112, December 1976.

[23] D. D. Beck and D. G. Wilson. *Gas-Turbine Regenerators*. Chapman & Hall, 1996.

[24] R. Prouty. *Helicopter Aerodynamics*. Eagle Eye Solutions, P.O. Box 46885, Cincinnati, OH, 54246, United States of America, 2007.

[25] W. Johnson. *Helicopter theory*. Dover publications, inc., 1994.

[26] J. Leishman. *Principles of Helicopter Aerodynamics.* Cambridge University Press, 2002.